

HARMamba: Efficient Wearable Sensor Human Activity Recognition Based on Bidirectional Selective SSM

Shuangjian Li, Tao Zhu, *Member, IEEE*, Furong Duan, Liming Chen *Senior Member, IEEE*, Huansheng Ning, *Senior Member, IEEE*, and Yaping Wan

Abstract—Wearable sensor human activity recognition (HAR) is a crucial area of research in activity sensing. While transformer-based temporal deep learning models have been extensively studied and implemented, their large number of parameters present significant challenges in terms of system computing load and memory usage, rendering them unsuitable for real-time mobile activity recognition applications. Recently, an efficient hardware-aware state space model (SSM) called Mamba has emerged as a promising alternative. Mamba demonstrates strong potential in long sequence modeling, boasts a simpler network architecture, and offers an efficient hardware-aware design. Leveraging SSM for activity recognition represents an appealing avenue for exploration. In this study, we introduce HARMamba, which employs a more lightweight selective SSM as the foundational model architecture for activity recognition. The goal is to address the computational resource constraints encountered in real-time activity recognition scenarios. Our approach involves processing sensor data flow by independently learning each channel and segmenting the data into "patches." The marked sensor sequence's position embedding serves as the input token for the bidirectional state space model, ultimately leading to activity categorization through the classification head. Compared to established activity recognition frameworks like Transformer-based models, HARMamba achieves superior performance while also reducing computational and memory overhead. Furthermore, our proposed method has been extensively tested on four public activity datasets: PAMAP2, WISDM, UNIMIB, and UCI, demonstrating impressive performance in activity recognition tasks.

Index Terms—Human Activity Recognition, Selective State Space Models, Wearable Sensors, Deep Learning

I. INTRODUCTION

THE utilization of deep learning and wearable sensors for real-time human activity recognition has emerged as a prominent research focus in recent years, holding significant promise for applications in medical health, assisted living, smart homes, and other domains. The Transformer model, renowned for its success in natural language processing (NLP) [1], computer vision (CV) [2], and time series analysis, stands

out for its attention mechanism, enabling automatic learning of relationships and correlations in sequences, thus proving advantageous for sequence modeling endeavors. Nonetheless, conventional Transformer-based models encounter challenges when handling extensive sequences of sensor data due to the quadratic time complexity of self-attention computation, which restricts the extraction of valuable information from individual time points. Moreover, these models often demand substantial training data, a limitation exacerbated in tasks like activity recognition where data scarcity hampers performance. To address these issues, numerous studies are investigating more efficient attention mechanisms [3], [4], albeit often at the expense of attention's effectiveness. Therefore, the quest for a novel architecture capable of accommodating long-term dependencies in sensor activity signals while ensuring linear computational resource utilization is paramount in the realm of activity recognition.

Recent research efforts [5], [6] have sparked significant interest in state space models (SSMs). Modern iterations of SSMs excel in capturing long-range dependencies effectively, and the incorporation of parallel training computations enables continuous enhancement over extended durations. These models exhibit a remarkable capability in modeling sequence dependencies. Various SSM-based methodologies have been introduced for applications in domains dealing with continuous signal data, notably the Linear State Space Layer (LSSL) [6], Structured State Space Sequence Model (S4) [5], Diagonal State Space (DSS) [7], and S4D [8]. Leveraging efficient convolution or recursion computations with linear or near-linear scalability concerning sequence length, these approaches prove versatile in processing sequence data across diverse tasks and modalities. Notably, the recent innovation of Mamba [9] introduced a straightforward selection mechanism to parameterize SSM parameters based on input, along with a hardware-aware algorithm that achieves highly efficient training and inference. However, the exploration of SSM-based backbone networks for processing IMU activity data (e.g., accelerometers, gyroscopes, magnetometers) remains an uncharted territory.

While Mamba has demonstrated success in modeling language, audio, video, and other domains, it encounters challenges when applied to sensor activity data due to its unidirectional modeling approach and lack of consideration for sequence position information. Inspired by [10], [11], we introduce the HARMamba model. Initially, we segment each

This work was supported in part by the National Natural Science Foundation of China(62006110), the Natural Science Foundation of Hunan Province (2021JJ30574). (Corresponding author: Tao Zhu.)

Shuangjian Li, Tao Zhu, Furong Duan and Yaping Wan are with the School of Computer Science, University of South China, 421001 China (e-mail: sjli@stu.usc.edu.cn, tzhu@usc.edu.cn, frduan@stu.usc.edu.cn, ypan@aliyun.com). Liming Chen was with School of Computer Science and Technology, Dalian University of Technology, China. Huansheng Ning was Department of Computer & Communication Engineering, University of Science and Technology Beijing, 100083 China (email: limingchen0922@dlut.edu.cn, ninghuansheng@ustb.edu.cn).

channel of continuous sensor data into patches, with each patch encapsulating sensor channel information. Subsequently, we apply position embedding to each patch block, projecting them as linear vectors into Mamba blocks. These Mamba blocks leverage bidirectional selective state space to efficiently compress patch sequence representations, with position embedding facilitating information exchange between patch blocks and enhancing the model's accuracy in activity recognition. Leveraging Mamba's linear modeling capability, HARMamba adopts a pure SSM approach, modeling IMU signals in patch form. Our method upholds the training parallelism of SSM, ensuring inference efficiency and achieving notable enhancements with a marginal increase in parameter count. This design establishes a versatile and efficient backbone network for activity recognition.

The main contributions of this paper can be summarized as follows:

- We introduced a simple and efficient framework called HARMamba, which is a pioneering approach that applies the choice state space model and scanning mechanism to activity recognition tasks.
- The framework adopts a sensor data channel-independent approach and patch operation to process sensor signal sequences, modeling the global context and location embedding of sensor signal patch sequences through bidirectional SSM.
- The framework we have proposed achieves efficient utilization of computational resources, with parameters, computational speed, and memory consumption surpassing Transformer-based frameworks. This characteristic facilitates its deployment on real-time activity recognition devices.
- Performing activity recognition classification experiments on four widely utilized benchmark datasets, the findings demonstrate that HARMamba demonstrates superior recognition performance when compared to alternative frameworks.

II. RELATED WORK

A. Sensor-based activity recognition

Sensor-based human activity recognition (HAR) research mainly relies on inertial measurement unit (IMU) sensors in wearable devices such as smart watches, smart insoles, and exercise bands. A common approach to sensor-based activity recognition involves utilizing fixed-size sliding windows, which has shown impressive results [12]. [13] proposed a long short-term memory (LSTM)-based classification method for identifying fine-grained patterns based on high-level features extracted from sequential motion data. [14] proposes a new deformable convolutional network for human activity recognition from complex sensory data. In the field of HAR, [15] introduced an attention-based multi-head model for human activity recognition. Similarly, [16] proposed a model based on the gated recurrent unit initialization (GRU-INC) model, which is an initial attention-based method that uses gated recurrent units (GRU) to effectively utilize spatiotemporal information.

time series data. Furthermore, [17] proposed a triplet cross-dimensional attention method for sensor-based activity recognition tasks, deploying three attention branches to capture the cross-interaction between sensor dimensions, time dimensions, and channel dimensions. Similarly, [18] introduced a novel multi-branch CNN that incorporates an attention mechanism to perform kernel selection among multiple branches with different receptive fields in the HAR domain. Furthermore, the multi-branch CNN-BiLSTM network proposed by [19] automatically extracts features from raw sensor data with minimal data preprocessing. [20] proposed an adaptive Transformer method that achieved good results on smartphone motion sensor data from a wide range of activities. [21] introduces a novel multi-window fusion method that involves segmenting the data using five different window sizes and fusing the recognition results in two stages. Inspired by the task of semantic segmentation of images, [22]–[25] applies FCN (fully convolutional network) and U-net to sensor-based activity recognition to predict dense labels, and achieves good recognition results. [26] further propose Conditional-UNet for coherent human activity recognition with multiple dense labels, explicitly modeling the conditional dependencies between these labels. [27] proposed a deep learning model Multi-ResAtt, which integrates recurrent neural networks with attention to extract time series features and perform activity recognition.

B. State space models

State Space Sequence Model (SSM) [5], [6], has become a promising architecture for sequence modeling. Mamba [9] introduces a selective SSM architecture, integrates time-varying parameters into the SSM framework, and proposes a hardware-aware algorithm to facilitate efficient training and inference processes. Some research works utilize SSM in computer vision to process 2D data. 2D SSM [27] introduces an SSM block at the beginning of each Transformer block [1], [2]. DenseMamba [28] By selectively integrating shallow hidden states into deeper layers, DenseSSM preserves fine-grained information that is critical to the final output. ConvSSM [29] integrates the tensor modeling principles of ConvLSTM [30] with SSM, illustrating the utilization of parallel scans in convolutional recursion. This approach enables sub-quadratic parallelization and fast autoregressive generation. Vim [10] introduces a bidirectional SSM block for efficient and general visual representation learning, achieving comparable performance to the established ViT [2] method. VMamba [31] The Cross Scan Module (CSM) is introduced, designed to traverse the spatial domain and convert any non-causal visual image into an ordered sequence of patches. This approach achieves linear complexity while maintaining the global receptive field. LightM-UNet [32] introduces lightweight Mamba UNet, which integrates Mamba and UNet in a lightweight framework. Motion Mamba [33] proposed a groundbreaking motion generation model using SSM, which designed a hierarchical temporal Mamba (HTM) block and a bidirectional spatial Mamba (BSM) block to process temporal data and bidirectional processing respectively. Latent pose data.

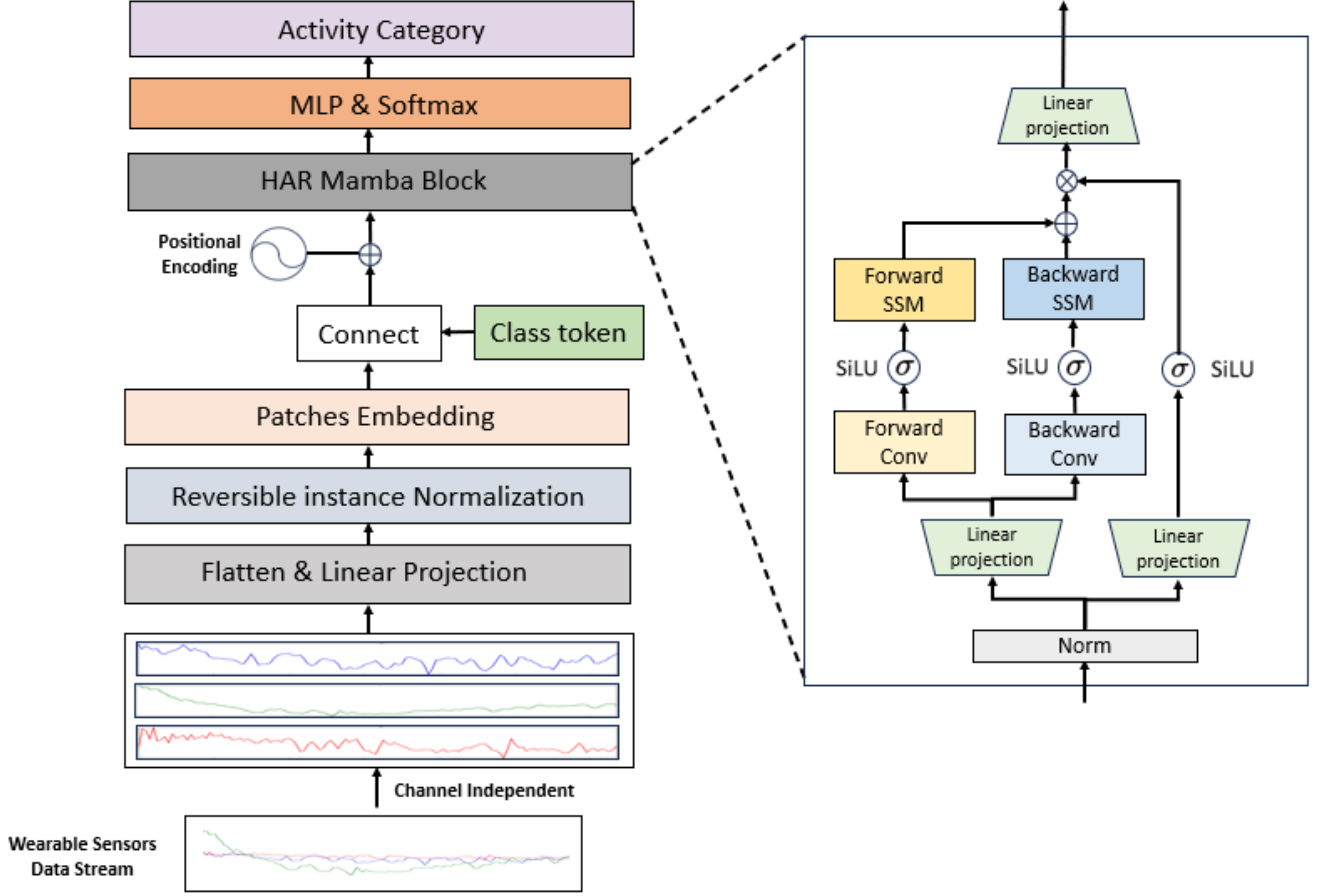


Fig. 1. illustrates the schematic of our proposed HARMamba model. Initially, we render the input sensor signal sequence channel-agnostic, segment the sequence of each channel into patch sequences, and subsequently map them to patch tokens while incorporating position encoding for each token. Subsequently, the token sequence is fed into the HARMamba architecture. In contrast to Mamba, which is tailored for text sequences, the HARMamba encoder executes bidirectional processing of token sequences.

III. METHOD

This section provides a detailed introduction to the HAR-Mamba architecture. Firstly, the basic concepts of SSM are presented, followed by an explanation of how the input token sequence is processed and the HARMamba model is utilized for activity recognition

A. Preliminaries

Inspired by the Structured State Space Sequence Model (S4) and Mamba, SSM has emerged as a promising architecture for efficient long sequence modeling. Structured SSM maps a sequence $x(t) \in \mathbb{R}^L$ to $y(t) \in \mathbb{R}^L$ by hiding the state $h(t) \in \mathbb{R}^N$, and the model uses $\mathbf{A} \in \mathbb{R}^{N \times N}$ as an evolution parameter and $\mathbf{B} \in \mathbb{R}^{N \times 1}$ and $\mathbf{C} \in \mathbb{R}^{1 \times N}$ as projection parameters. The whole process can be formulated as:

$$\begin{aligned} h'(t) &= \mathbf{A}h(t) + \mathbf{B}h(t) \\ y(t) &= \mathbf{C}h(t) \end{aligned} \quad (1)$$

To apply SSM to discrete data, the continuous parameters \mathbf{A} and \mathbf{B} are converted into discrete parameters $\bar{\mathbf{A}}$ and $\bar{\mathbf{B}}$ using the

time scale parameter Δ . One commonly used transformation method is the zero-order hold (ZOH), which is defined as follows:

$$\begin{aligned} \bar{\mathbf{A}} &= \exp(\Delta\mathbf{A}) \\ \bar{\mathbf{B}} &= (\Delta\mathbf{A})^{-1}(\exp(\Delta\mathbf{A}) - I) \cdot \Delta\mathbf{B} \end{aligned} \quad (2)$$

After discretizing the parameters, the Eq. (1) can be rewritten using the discretization parameters as follows:

$$\begin{aligned} h_t &= \bar{\mathbf{A}}h_{t-1} + \bar{\mathbf{B}}x_t \\ y_t &= \mathbf{C}h_t \end{aligned} \quad (3)$$

The model calculates the output using global convolution:

$$\begin{aligned} \bar{\mathbf{K}} &= (\mathbf{C}\bar{\mathbf{B}}, \mathbf{C}\bar{\mathbf{A}}\bar{\mathbf{B}}, \dots, \mathbf{C}\bar{\mathbf{A}}^{M-1}\bar{\mathbf{B}}) \\ y &= \mathbf{x} * \bar{\mathbf{K}} \end{aligned} \quad (4)$$

The length of the input sequence \mathbf{x} is denoted by M , and the structured convolution kernel is represented by $\bar{\mathbf{K}} \in \mathbb{R}^M$. Eq. (3) is utilized for autoregressive inference of the model, while Eq. (4) is effective for parallel training.

B. HAR Mamba

Figure 1 shows the definition of the D_c -dimensional input wearable sensor sequence as $\mathbf{X}_{1:L} = [x_1, \dots, x_L], x_i \in \mathbb{R}^{D_c}$. Here, x_i represents the sensor signal collected at timestamp t , and the activity label corresponding to each sample is marked as $y_{1:L} = [y_1, \dots, y_L], y_t \in \mathbb{R}^C$. C represents the category of the activity number, t is the time step, L is the length of the wearable sensor sequence, and the length of Patch is defined as P .

The input sensor sequence $[x_1, \dots, x_L]$ is first divided into D_c single-variable sequences $x^{(i)} \in \mathbb{R}^{1 \times L}$. Prior to processing the patches, we apply reversible instance normalization (RevIN) [34] to multiple channels of sensor signal data. This is intended to address the issue of non-uniform time distribution between training and test data, which is often referred to as distribution shift. Before combining the channel modules, we normalize the data for each channel using instance normalization. For each instance of $x^{(i)}$, we compute the mean and standard deviation.

$$RevIN(x^{(i)}) = \left\{ \gamma_i \frac{x^{(i)} - Mean(x^{(i)})}{\sqrt{Var(x^{(i)}) + \varepsilon}} \right\}, i = 1, 2, \dots, D_c \quad (5)$$

After normalization of reversible instances, Each single-channel sensor signal sequence $x^{(i)}$ can be further divided into overlapping or non-overlapping Patch blocks, with a length of P . The non-overlapping part between two consecutive Patch blocks is referred to as the step size, expressed as S . The segmentation of the patch block results in a patch-level sensor sequence $x_p^{(i)} \in \mathbb{R}^{P \times N}$, where $N = \lfloor \frac{L-P}{S} \rfloor$. To represent the entire sensor sequence, denoted as $token_{cls}$, we use a class token which we splice to the end of the Patch sequence. Then, we linearly project $x_p^{(i)}$ onto a vector of size D and add a position embedding $E_{pos} \in \mathbb{R}^{(N+1) \times D}$. The expression for the position embedding is as follows:

$$\mathbf{T}_0 = [x_p^{(i)} \mathbf{W}, token_{cls}] + E_{pos} \quad (6)$$

Where $\mathbf{W} \in \mathbb{R}^{(N \times M) \times D}$ is the learnable projection matrix, then we input the token sequence representation \mathbf{T}_{l-1} into the HARMamba Block of the l -th layer, and the output is \mathbf{T}_l . We normalize the output class token \mathbf{T}_l^{N+1} and then transport it to the MLP. Finally, the final activity class prediction \hat{y} is obtained through the Softmax layer. The specific representation is as follows:

$$\mathbf{T}_l = HARMambaBlock(\mathbf{T}_{l-1}) \quad (7)$$

$$\hat{y} = Softmax(MLP(Norm(\mathbf{T}_l^{N+1}))) \quad (8)$$

Predicted and true labels are used to construct an activity classification loss, which efficiently optimizes model parameters. The loss is defined as follows:

$$L_{cls}(\hat{y}, y) = -\frac{1}{L} \sum_{l=1}^L \sum_{c=1}^C y \log(\hat{y}) \quad (9)$$

C. HARMamba Block

This section introduces the HARMamba Block, which models sensor sequences bidirectionally. The HARMamba Block is depicted in Figure 1.

The token sequence representation \mathbf{T}_{l-1} is normalized using a normalization layer. The output sequence is then projected into \mathbf{x} and \mathbf{z} of size E through two linear mappings.

$$\mathbf{x}, \mathbf{z} = Linear(Norm(\mathbf{T}_{l-1})) \quad (10)$$

The input \mathbf{x} is processed through two independent branches, one forward and one backward. In each direction, \mathbf{x} undergoes one-dimensional causal convolution resulting in \mathbf{x}'_o . The SiLU activation function is then applied to \mathbf{x}'_o before it is fed into the SSM. Within the SSM, \mathbf{x}'_o is linearly projected onto \mathbf{B}_o , \mathbf{C}_o , and Δ_o , and then converted through Δ_o to obtain $\overline{\mathbf{A}}_o$ and $\overline{\mathbf{B}}_o$. Finally, $y_{forward}$ and $y_{backward}$ are obtained through bidirectional SSM.

$$y_{forward/backward} = SSM(SiLU(Conv1D(\mathbf{x}))) \quad (11)$$

Finally, we add $y_{forward}$ and $y_{backward}$, calculate the result with \mathbf{z} to get the gate value, and then use it through a linear projection to get the final output Token sequence \mathbf{T}_l .

$$\mathbf{T}_l = Linear((y_{forward} + y_{backward}) \otimes \mathbf{z}) \quad (12)$$

Algorithm 1 describes the specific process. l represents the number of HARMamba Blocks, D represents the hidden state dimension, and E represents the extended state dimension.

Algorithm 1 HARMamba Block

Input: Patch token sequence $\mathbf{T}_{l-1} : (B, M, D)$

Output: Patch token sequence $\mathbf{T}_l : (B, M, D)$

- 1: $\mathbf{T}'_{l-1} : (B, M, D) \leftarrow \mathbf{Norm}(\mathbf{T}_{l-1})$
 - 2: $\mathbf{x}, \mathbf{z} : (B, M, E) \leftarrow \mathbf{Linear}(\mathbf{T}'_{l-1})$
 - 3: **for** o in $\{forward, backward\}$ **do**
 - 4: $\mathbf{x}'_o : (B, M, E) \leftarrow \mathbf{SiLU}(\mathbf{Conv1D}(\mathbf{x}))$
 - 5: $\mathbf{B}_o, \mathbf{C}_o, \Delta_o \leftarrow \mathbf{Linear}(\mathbf{x}'_o)$
 - 6: $\overline{\mathbf{A}}_o, \overline{\mathbf{B}}_o : Transform \mathbf{A}, \mathbf{B} \text{ through } \Delta_o$
 - 7: $\mathbf{y}_o : (B, M, E) \leftarrow \mathbf{SSM}(\overline{\mathbf{A}}_o, \overline{\mathbf{B}}_o, \mathbf{C}_o)$
 - 8: **end for**
 - 9: $\mathbf{T}_l \leftarrow \mathbf{Linear}((\mathbf{y}_{forward} + \mathbf{y}_{backward}) \odot \mathbf{SiLU}(\mathbf{z}))$
 - 10: **Return:** \mathbf{T}_l
-

IV. EXPERIMENT

This section introduces the experimental settings, datasets, recognition metrics, and competing algorithms used in the experiments. The proposed HARMamba framework is then evaluated using cutting-edge research, demonstrating significant advantages in recognition performance.

A. Experimental setup

The method was implemented using PyTorch and trained on two RTX 3090 GPUs. The batch size was set to 64, and AdamW with a momentum of 0.9 and a weight decay of 0.05 was used to optimize the model, along with a learning rate of 0.0001. The HARMamba block consists of 24 layers. The patch sizes for PAMAP2, UCI, UNIMIB HAR, and WISDM are 16, 16, 10, and 10 respectively.

B. Datasets

To evaluate our proposed method, we used four challenging public HAR datasets: WISDM, PAMAP 2, UNIMIB SHAR, and UCI. The datasets are briefly introduced below, and Table I provides details of the four benchmark datasets.

WISDM dataset [35]: this dataset was collected from 29 participants who wore mobile phones equipped with three-axis accelerometers in their pants pockets. The data were sampled at 20 Hz. The study participants engaged in six activities daily: walking, strolling, ascending stairs, descending stairs, standing, and standing still. To address any missing data in the dataset, the corresponding column’s mean is used for filling.

PAMAP2 dataset [36]: this dataset comprises data collected from nine participants wearing IMUs on their chest, hands, and ankles. These IMUs gather information on acceleration, angular velocity, and magnetic sensors. Each participant completed 12 mandatory activities, including lying down, standing, and going up and down stairs, as well as 6 optional activities, such as watching TV, driving a car, and playing ball.

UNIMIB SHAR dataset [37]: this dataset was collected by researchers at Milan-Bicocca. Thirty volunteers, aged 18 to 60, had their Samsung phones equipped with Bosch BMA 220 sensors. The study recorded 11,771 activities by placing phones in the participants’ left and right pockets. The dataset comprises 17 categories of activities, divided into two groups: 9 activities of daily living (ADL) and 8 falling behaviors.

UCI Dataset [38]: this dataset was collected from 30 volunteers aged 19 to 48 who strapped their smartphones to their waists and performed one of 6 standard activities using mobile phone software to record exercise data. The recorded motion data consists of linear acceleration (x, y, and z accelerometer data) and angular velocity (gyroscope data) from a Samsung Galaxy S II smartphone. The data was sampled at a frequency of 50Hz, which equates to 50 data points per second.

TABLE I
SPECIFICS OF THE BASELINE DATA SET

Dataset	Categories	Subject	Rate	Sample
WISDM	6	29	20HZ	1,098,208
PAMAP2	12	9	33.3HZ	2,872,533
UNIMIB HAR	17	4	30HZ	11,771
UCI	6	20	50HZ	74,8406

C. Evaluation metrics

To assess the activity categories of the final output of the model, we employ the following identification metrics:

Accuracy: an overall measure of correctness across all categories, calculated as follows:

$$Accuracy = \frac{\sum_{c=1}^C TP_c + \sum_{c=1}^C TN_c}{\sum_{c=1}^C (TP_c + TN_c + FP_c + FN_c)} \quad (13)$$

Weighted F1 score: The weighted F1 score is calculated based on the proportion of samples:

$$F_w = \sum_{c=1}^C 2 * w_c \frac{prec_c \cdot recall_c}{prec_c + recall_c} \quad (14)$$

Where $prec_c = \frac{TP_c}{TP_c + FP_c}$ and $recall_c = \frac{TP_c}{TP_c + FN_c}$ represent precision and recall, respectively. The weight w_c is calculated as the ratio of n_c to N , where n_c is the number of Patch samples per class, and N is the total number of samples.

D. Comparisons with activity recognition algorithm

This subsection compares the recognition performance of the proposed model with state-of-the-art competing methods on four public wearable device-based HAR datasets. Our method achieves results comparable to or better than the state-of-the-art on every public dataset. The results are presented in Table II.

The HARMamba block module was replaced with the Transformer architecture, and the performance of both models was evaluated on four datasets, including the number of model parameters and FLOPs. Table III presents the comparison results between the two models. On four datasets, HARMamba has fewer parameters than the Transformer model, but it has higher FLOPs with the same patch size.

To evaluate the efficiency of HARMamba in activity recognition tasks, we benchmarked GPU memory on the PAMAP2 dataset using different patch sizes. Figure 2 shows that we replaced the HARMamba module with the Transformer module to use memory resources. HARMamba has excellent linear scaling performance and consumes fewer computing resources than the Transformer model.

E. Ablation experiment

This section examines the impact of bidirectional SSM on classification results. Three strategies are mainly studied: 1) SSM: using a single Mamba block to process the sensor data representation sequence directly. 2) Bidirectional SSM: adding an additional SSM to each block to handle the sequence of sensor data representations in the backward direction. 3) Bidirectional SSM + Conv1d: adding a Conv1d before each SSM based on Bidirectional SSM.

As shown in Table IV, Optimal performance is achieved by adding additional backward SSM and Conv 1d. This also leads to better classification results based on a single Mamba block. The default strategy in the HARMamba block is to use the bidirectional SSM+Conv1d.

TABLE II
ACC AND F1 PERFORMANCE ON FOUR PUBLIC DATASETS

Dataset	Related work	Method	Accuracy	F1 score
PAMAP2	Essa E et al. (2023) [39]	Temporal-channel convolution with self-attention network	89.10%	0.8642
	Tang Y et al. (2022) [17]	Triple cross domain Attention	-	0.9320
	Tang Y et al. (2022) [40]	Dual-branch interactive networks on multichannel	92.05%	0.9199
	Huang W et al. (2023) [41]	Channel-Equalization-HAR	92.14%	0.9218
	Tang Y et al. (2022) [42]	HS-ResNet	93.75%	0.9429
	Challa S K et al. (2022) [19]	CNN-BiLSTM	94.29%	0.9427
	F. Duan et al. (2023) [43]	MTHAR	94.50%	0.9480
	Tong L et al. (2022) [44]	Bi-GRU-I	95.42%	0.9545
	J Li et al. (2023) [45]	Multi-resolution Fusion Convolutional Network	<u>98.14%</u>	<u>0.9812</u>
	Ours	HARMamba	99.91%	0.9974
UCI	MA Khatun et al. (2022) [46]	CNN-LSTM with Self-Attention	93.11%	0.8961
	Y Wang et al. (2023) [47]	Multifeature extraction framework based on attention mechanism	96.00%	0.9580
	F. Duan et al. (2023) [43]	MTHAR	96.32%	<u>0.9723</u>
	Challa S K et al. (2022) [19]	CNN-BiLSTM	96.37%	0.9631
	Tang Y et al. (2022) [42]	HS-ResNet	97.28%	0.9738
	Tang Y et al. (2022) [17]	Triple cross domain Attention	-	0.9677
	Huang W et al. (2023) [41]	Channel-Equalization-HAR	<u>97.35%</u>	0.9712
		Ours	HARMamba	97.65%
UNIMIB HAR	F. Duan et al. (2023) [43]	MTHAR	76.48%	0.7571
	Huang W et al. (2023) [41]	Channel-Equalization-HAR	78.65%	0.7878
	Tang Y et al. (2022) [42]	HS-ResNet	79.02%	0.7919
	Tang Y et al. (2022) [17]	Triple cross domain Attention	-	0.7855
	MAA Al-Qaness et al. (2023) [48]	Multilevel Residual Network With Attention	<u>85.35%</u>	<u>0.8506</u>
		Ours	HARMamba	88.08%
WISDM	Essa E et al. (2023) [39]	Temporal-channel convolution with self-attention network	92.51%	0.8518
	Tang Y et al. (2022) [17]	Triple cross domain Attention	-	0.9861
	Challa S K et al. (2022) [19]	CNN-BiLSTM	96.05%	0.9604
	Y Wang et al. (2023) [47]	Multifeature extraction framework based on attention mechanism	97.90%	0.9800
	Tong L et al. (2022) [44]	Bi-GRU-I	98.25%	0.9712
	J Li et al. (2023) [45]	Multi-resolution Fusion Convolutional Network	<u>98.60%</u>	<u>0.9864</u>
	Tang Y et al. (2022) [40]	Dual-branch interactive networks on multichannel	98.17%	0.9856
	Huang W et al. (2023) [41]	Channel-Equalization-HAR	99.04%	0.9918
	Ours	HARMamba	98.25%	0.9838

TABLE III
ON FOUR DATASETS, COMPARE THE NUMBER OF PARAMETERS AND FLOPS BETWEEN THE HARMAMBA AND TRANSFORMER ARCHITECTURES.

Method	Sequence size	param.(M)	FLOPs(M)
PAMAP2			
Transformer	512	3.3060	211.06
HARMamba	512	0.7966	279.21
UCI			
Transformer	128	2.5057	197.91
HARMamba	128	0.7880	237.83
UNIMIB HAR			
Transformer	151	2.4637	162.26
HARMamba	151	0.7883	238.36
WISDM			
Transformer	200	2.4796	219.71
HARMamba	200	0.7877	256.52

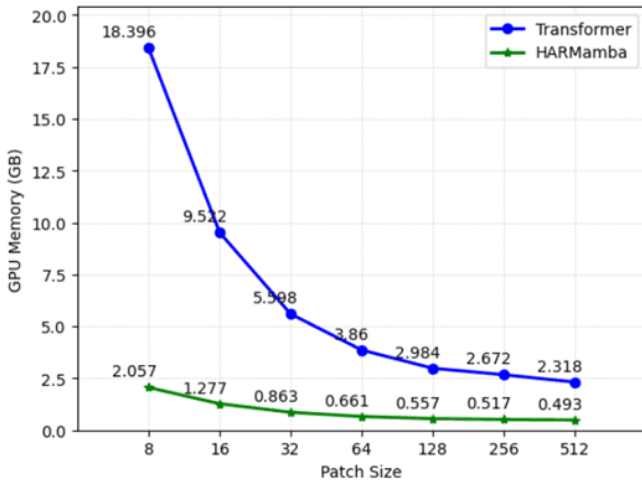


Fig. 2. The memory efficiency results of Transformer and HARMamba models are compared under different patch sizes on the Pamap2 dataset.

TABLE IV
THE IMPACT OF DIFFERENT STRATEGIES ON THE RESULTS ON THE UNIMIBHAR DATASET

Strategy	Accuracy	F1 score
SSM	77.30%	0.7723
Bidirectional SSM	83.10%	0.8292
Bidirectional SSM + Conv1d	88.08%	0.8823

V. CONCLUSION AND FUTURE WORK

We introduce HARMamba, a lightweight activity recognition model that employs the state-of-the-art Mamba architecture as its backbone. By implementing bidirectional state space modeling on sensor patch blocks, HARMamba outperforms attention-based and convolutional networks in terms of recognition accuracy while maintaining lower computational complexity and memory consumption. This demonstrates its potential as a favorable backbone for activity recognition tasks, with plans for future extensions. Specifically, we aim to apply Mamba in self-supervised learning to alleviate the need for active labeling, explore cross-human domain adaptation, and deploy the model on mobile devices for real-time activity recognition.

REFERENCES

- [1] A. Waswani, N. Shazeer, N. Parmar, J. Uszkoreit, L. Jones, A. Gomez, L. Kaiser, and I. Polosukhin, "Attention is all you need," in *NIPS*, 2017.
- [2] A. Dosovitskiy, L. Beyer, A. Kolesnikov, D. Weissenborn, X. Zhai, T. Unterthiner, M. Dehghani, M. Minderer, G. Heigold, S. Gelly, J. Uszkoreit, and N. Houlsby, "An image is worth 16x16 words: Transformers for image recognition at scale," *ICLR*, 2021.
- [3] Z. Liu, Y. Lin, Y. Cao, H. Hu, Y. Wei, Z. Zhang, S. Lin, and B. Guo, "Swin transformer: Hierarchical vision transformer using shifted windows," in *Proceedings of the IEEE/CVF international conference on computer vision*, 2021, pp. 10012–10022.
- [4] Z. Xia, X. Pan, S. Song, L. E. Li, and G. Huang, "Vision transformer with deformable attention," in *Proceedings of the IEEE/CVF conference on computer vision and pattern recognition*, 2022, pp. 4794–4803.
- [5] A. Gu, K. Goel, and C. Ré, "Efficiently modeling long sequences with structured state spaces," *arXiv preprint arXiv:2111.00396*, 2021.
- [6] A. Gu, I. Johnson, K. Goel, K. Saab, T. Dao, A. Rudra, and C. Ré, "Combining recurrent, convolutional, and continuous-time models with linear state space layers," *Advances in neural information processing systems*, vol. 34, pp. 572–585, 2021.
- [7] A. Gupta, A. Gu, and J. Berant, "Diagonal state spaces are as effective as structured state spaces," *Advances in Neural Information Processing Systems*, vol. 35, pp. 22982–22994, 2022.
- [8] A. Gu, K. Goel, A. Gupta, and C. Ré, "On the parameterization and initialization of diagonal state space models," *Advances in Neural Information Processing Systems*, vol. 35, pp. 35971–35983, 2022.
- [9] A. Gu and T. Dao, "Mamba: Linear-time sequence modeling with selective state spaces," *arXiv preprint arXiv:2312.00752*, 2023.
- [10] L. Zhu, B. Liao, Q. Zhang, X. Wang, W. Liu, and X. Wang, "Vision mamba: Efficient visual representation learning with bidirectional state space model," *arXiv preprint arXiv:2401.09417*, 2024.
- [11] Y. Nie, N. H. Nguyen, P. Sinthong, and J. Kalagnanam, "A time series is worth 64 words: Long-term forecasting with transformers," in *International Conference on Learning Representations*, 2023.
- [12] K. Chen, D. Zhang, L. Yao, B. Guo, Z. Yu, and Y. Liu, "Deep learning for sensor-based human activity recognition: Overview, challenges, and opportunities," *ACM Computing Surveys (CSUR)*, vol. 54, no. 4, pp. 1–40, 2021.
- [13] X. Zhou, W. Liang, K. I.-K. Wang, H. Wang, L. T. Yang, and Q. Jin, "Deep-learning-enhanced human activity recognition for internet of healthcare things," *IEEE Internet of Things Journal*, vol. 7, no. 7, pp. 6429–6438, 2020.
- [14] S. Xu, L. Zhang, W. Huang, H. Wu, and A. Song, "Deformable convolutional networks for multimodal human activity recognition using wearable sensors," *IEEE Transactions on Instrumentation and Measurement*, vol. 71, pp. 1–14, 2022.
- [15] Z. N. Khan and J. Ahmad, "Attention induced multi-head convolutional neural network for human activity recognition," *Applied soft computing*, vol. 110, p. 107671, 2021.
- [16] T. R. Mim, M. Amatullah, S. Afreen, M. A. Yousuf, S. Uddin, S. A. Alyami, K. F. Hasan, and M. A. Moni, "Gru-inc: An inception-attention based approach using gru for human activity recognition," *Expert Systems with Applications*, vol. 216, p. 119419, 2023.

- [17] Y. Tang, L. Zhang, Q. Teng, F. Min, and A. Song, "Triple cross-domain attention on human activity recognition using wearable sensors," *IEEE Transactions on Emerging Topics in Computational Intelligence*, vol. 6, no. 5, pp. 1167–1176, 2022.
- [18] W. Gao, L. Zhang, W. Huang, F. Min, J. He, and A. Song, "Deep neural networks for sensor-based human activity recognition using selective kernel convolution," *IEEE Transactions on Instrumentation and Measurement*, vol. 70, pp. 1–13, 2021.
- [19] S. K. Challa, A. Kumar, and V. B. Semwal, "A multibranch cnn-bilstm model for human activity recognition using wearable sensor data," *The Visual Computer*, vol. 38, no. 12, pp. 4095–4109, 2022.
- [20] I. Dirgová Luptáková, M. Kubovčík, and J. Pospíchal, "Wearable sensor-based human activity recognition with transformer model," *Sensors*, vol. 22, no. 5, p. 1911, 2022.
- [21] O. Banos, J.-M. Galvez, M. Damas, A. Guillen, L.-J. Herrera, H. Pomares, I. Rojas, C. Villalonga, C. S. Hong, and S. Lee, "Multiwindow fusion for wearable activity recognition," in *Advances in Computational Intelligence: 13th International Work-Conference on Artificial Neural Networks, IWANN 2015, Palma de Mallorca, Spain, June 10-12, 2015. Proceedings, Part II 13*. Springer, 2015, pp. 290–297.
- [22] J. Long, E. Shelhamer, and T. Darrell, "Fully convolutional networks for semantic segmentation," in *Proceedings of the IEEE conference on computer vision and pattern recognition*, 2015, pp. 3431–3440.
- [23] V. Badrinarayanan, A. Kendall, and R. Cipolla, "Segnet: A deep convolutional encoder-decoder architecture for image segmentation," *IEEE transactions on pattern analysis and machine intelligence*, vol. 39, no. 12, pp. 2481–2495, 2017.
- [24] R. Yao, G. Lin, Q. Shi, and D. C. Ransinghe, "Efficient dense labelling of human activity sequences from wearables using fully convolutional networks," *Pattern Recognition*, vol. 78, pp. 252–266, 2018.
- [25] Y. Zhang, Z. Zhang, Y. Zhang, J. Bao, Y. Zhang, and H. Deng, "Human activity recognition based on motion sensor using u-net," *IEEE Access*, vol. 7, pp. 75 213–75 226, 2019.
- [26] L. Zhang, W. Zhang, and N. Japkowicz, "Conditional-unet: A condition-aware deep model for coherent human activity recognition from wearables," in *2020 25th International Conference on Pattern Recognition (ICPR)*. IEEE, 2021, pp. 5889–5896.
- [27] E. Baron, I. Zimmerman, and L. Wolf, "2-d ssm: A general spatial layer for visual transformers," *arXiv preprint arXiv:2306.06635*, 2023.
- [28] W. He, K. Han, Y. Tang, C. Wang, Y. Yang, T. Guo, and Y. Wang, "DenseMamba: State space models with dense hidden connection for efficient large language models," *arXiv preprint arXiv:2403.00818*, 2024.
- [29] J. Smith, S. De Mello, J. Kautz, S. Linderman, and W. Byeon, "Convolutional state space models for long-range spatiotemporal modeling," *Advances in Neural Information Processing Systems*, vol. 36, 2024.
- [30] X. Shi, Z. Chen, H. Wang, D.-Y. Yeung, W.-K. Wong, and W.-c. Woo, "Convolutional lstm network: A machine learning approach for precipitation nowcasting," *Advances in neural information processing systems*, vol. 28, 2015.
- [31] Y. Liu, Y. Tian, Y. Zhao, H. Yu, L. Xie, Y. Wang, Q. Ye, and Y. Liu, "Vmamba: Visual state space model," *arXiv preprint arXiv:2401.10166*, 2024.
- [32] W. Liao, Y. Zhu, X. Wang, C. Pan, Y. Wang, and L. Ma, "Lightm-unet: Mamba assists in lightweight unet for medical image segmentation," *arXiv preprint arXiv:2403.05246*, 2024.
- [33] Z. Zhang, A. Liu, I. Reid, R. Hartley, B. Zhuang, and H. Tang, "Motion mamba: Efficient and long sequence motion generation with hierarchical and bidirectional selective ssm," *arXiv preprint arXiv:2403.07487*, 2024.
- [34] T. Kim, J. Kim, Y. Tae, C. Park, J.-H. Choi, and J. Choo, "Reversible instance normalization for accurate time-series forecasting against distribution shift," in *International Conference on Learning Representations*, 2021.
- [35] J. R. Kwapisz, G. M. Weiss, and S. A. Moore, "Activity recognition using cell phone accelerometers," *ACM SigKDD Explorations Newsletter*, vol. 12, no. 2, pp. 74–82, 2011.
- [36] A. Reiss and D. Stricker, "Introducing a new benchmarked dataset for activity monitoring," in *2012 16th international symposium on wearable computers*. IEEE, 2012, pp. 108–109.
- [37] D. Micucci, M. Mobilio, and P. Napolitano, "Unimib shar: A dataset for human activity recognition using acceleration data from smartphones," *Applied Sciences*, vol. 7, no. 10, p. 1101, 2017.
- [38] D. Anguita, A. Ghio, L. Oneto, X. Parra Perez, and J. L. Reyes Ortiz, "A public domain dataset for human activity recognition using smartphones," in *Proceedings of the 21th international European symposium on artificial neural networks, computational intelligence and machine learning*, 2013, pp. 437–442.
- [39] E. Essa and I. R. Abdelmaksoud, "Temporal-channel convolution with self-attention network for human activity recognition using wearable sensors," *Knowledge-Based Systems*, vol. 278, p. 110867, 2023.
- [40] Y. Tang, L. Zhang, H. Wu, J. He, and A. Song, "Dual-branch interactive networks on multichannel time series for human activity recognition," *IEEE Journal of Biomedical and Health Informatics*, vol. 26, no. 10, pp. 5223–5234, 2022.
- [41] W. Huang, L. Zhang, H. Wu, F. Min, and A. Song, "Channel-equalization-har: A light-weight convolutional neural network for wearable sensor based human activity recognition," *IEEE Transactions on Mobile Computing*, vol. 22, no. 9, pp. 5064–5077, 2023.
- [42] Y. Tang, L. Zhang, F. Min, and J. He, "Multiscale deep feature learning for human activity recognition using wearable sensors," *IEEE Transactions on Industrial Electronics*, vol. 70, no. 2, pp. 2106–2116, 2022.
- [43] F. Duan, T. Zhu, J. Wang, L. Chen, H. Ning, and Y. Wan, "A multi-task deep learning approach for sensor-based human activity recognition and segmentation," *IEEE Transactions on Instrumentation and Measurement*, 2023.
- [44] L. Tong, H. Ma, Q. Lin, J. He, and L. Peng, "A novel deep learning bi-gru-i model for real-time human activity recognition using inertial sensors," *IEEE Sensors Journal*, vol. 22, no. 6, pp. 6164–6174, 2022.
- [45] J. Li, H. Xu, and Y. Wang, "Multi-resolution fusion convolutional network for open set human activity recognition," *IEEE Internet of Things Journal*, 2023.
- [46] M. A. Khatun, M. A. Yousuf, S. Ahmed, M. Z. Uddin, S. A. Alyami, S. Al-Ashhab, H. F. Akhdar, A. Khan, A. Azad, and M. A. Moni, "Deep cnn-lstm with self-attention model for human activity recognition using wearable sensor," *IEEE Journal of Translational Engineering in Health and Medicine*, vol. 10, pp. 1–16, 2022.
- [47] Y. Wang, H. Xu, Y. Liu, M. Wang, Y. Wang, Y. Yang, S. Zhou, J. Zeng, J. Xu, S. Li *et al.*, "A novel deep multifeature extraction framework based on attention mechanism using wearable sensor data for human activity recognition," *IEEE Sensors Journal*, vol. 23, no. 7, pp. 7188–7198, 2023.
- [48] M. A. Al-Qaness, A. Dahou, M. Abd Elaziz, and A. Helmi, "Multi-resatt: Multilevel residual network with attention for human activity recognition using wearable sensors," *IEEE Transactions on Industrial Informatics*, vol. 19, no. 1, pp. 144–152, 2023.